

Stent deformation, physical stress, and drug elution obtained with provisional stenting, conventional culotte and Tryton-based culotte to treat bifurcations: a virtual simulation study

Stefano Morlacchi¹, PhD; Claudio Chiastra¹, M.Eng; Elena Cutri^{1,2}, PhD; Paolo Zunino^{2,3}, PhD; Francesco Burzotta⁴, MD; Luca Formaggia², PhD; Gabriele Dubini¹, PhD; Francesco Migliavacca^{1*}, PhD

1. Laboratory of Biological Structure Mechanics (LaBS), Department of Chemistry, Materials and Chemical Engineering “Giulio Natta”, Politecnico di Milano, Milan, Italy; 2. Modelling and Scientific Computing (MOX), Department of Mathematics, Politecnico di Milano, Milan, Italy; 3. Department of Mechanical Engineering and Materials Science, University of Pittsburgh, Pittsburgh, PA, USA; 4. Department of Cardiovascular Medicine, Università Cattolica del Sacro Cuore, Rome, Italy

The accompanying supplementary data are published online at: http://www.pcronline.com/eurointervention/71st_issue/242

KEYWORDS

- coronary bifurcations
- dedicated stents
- drug-eluting stents
- finite element analysis

Abstract

Aims: This study sought to investigate the possible influence of different bifurcation stenting techniques on stent deformation, physical stress, and drug elution using a virtual tool that includes structural, fluid dynamics and drug-eluting numerical models.

Methods and results: A virtual bench test based on explicit dynamics modelling was used to simulate procedures on bifurcated coronary vessels performed according to three different stenting techniques: provisional side branch stenting, culotte, and Tryton-based culotte. Geometrical configurations obtained after virtual stenting simulations were used to perform fluid dynamics and drug elution analyses. The results showed that substantially different patterns of mechanical deformation, shear stress and theoretical drug elution were obtained using the different techniques. Compared with conventional culotte, the dedicated Tryton seems to facilitate the intervention in terms of improved access to the main branch and to lower its biomechanical influence on the coronary bifurcation in terms of mechanical and haemodynamic parameters. However, since the Tryton stent is a bare metal stent, the drug elution obtained is lower.

Conclusions: Numerical models might successfully complement the information on stenting procedures obtained with traditional approaches such as *in vitro* bench testing or clinical trials. Devices dedicated to bifurcations may facilitate procedure completion and may result in specific patterns of mechanical stress, regional blood flow and drug elution.

*Corresponding author: Laboratory of Biological Structure Mechanics, Department of Chemistry, Materials and Chemical Engineering “Giulio Natta”, Politecnico di Milano, Piazza Leonardo da Vinci, 32, 20133 Milan, Italy. E-mail: francesco.migliavacca@polimi.it

Abbreviations

BMS	bare metal stent
CFD	computational fluid dynamics
DES	drug-eluting stent
FKB	final kissing balloon
MB	main branch
OSI	oscillatory shear index
PEEQ	plastic equivalent deformation
RRT	relative residence time
SB	side branch
TAWSS	time-averaged wall shear stress
WSS	wall shear stress

Introduction

Despite recent technical and clinical improvements, bifurcated coronary artery lesions still remain an open challenge for interventional cardiologists performing percutaneous coronary interventions. The “optimal” procedure of stent implantation in bifurcated lesions has still not been defined but should theoretically restore both main branch (MB) and side branch (SB) patency, avoiding major myocardial injury and allowing a simple and straight execution. Among the different controversies relating to the optimal technique, a major issue is the choice between a single- and a double-stenting approach. At present, available clinical data on bare metal stents (BMS) and drug-eluting stents (DES) suggest that simple strategies are associated with lower rates of adverse clinical events, while increased procedure duration, fluoroscopy times and contrast volume affect complex strategies. As a consequence, in most cases a single-stent provisional technique should be considered as the preferred strategy¹. However, such evidence stems from studies using standard DES and may be challenged by novel technical innovations such as stents dedicated to bifurcations². These devices may provide new treatment options by solving a series of technical problems relating to the implantation of regular stents in bifurcated lesions. Among the different dedicated devices, the Tryton side branch stent (Tryton Medical, Durham, NC, USA), has been clinically tested obtaining promising results^{3,4}. It is a balloon-expandable cobalt-chromium BMS characterised by three different specific designs which are designed to facilitate the culotte technique.

During the evaluation of novel interventional devices, virtual modelling techniques based on numerical methods are emerging as a valuable tool for the assessment of several mechanical (arterial wall and stent strut stresses)⁵⁻⁸ and haemodynamic variables (shear stresses, drug release)⁹⁻¹² which are hardly detectable by means of *in vitro* or *in vivo* experiments. Novel evidence obtained through these methods might be used by physicians to complement the information coming from traditional studies, especially in the case of new dedicated devices or particular techniques where large randomised trials are currently lacking mainly due to high costs and duration.

Accordingly, an innovative virtual tool that includes structural¹³, computational fluid dynamics (CFD)^{14,15} and drug-eluting¹⁶ numerical models was implemented in this study, using both commercial and in-house developed software. In particular, the present study

aimed to assess the biomechanical influence provoked by three different stenting procedures: provisional side branch (PSB) stenting, a standard stent-based (“conventional”) culotte and a Tryton-based culotte. The geometrical configurations of stents and arteries obtained through the virtual stent deployments were then used to create more realistic blood volumes for the CFD and drug elution studies. Results of the simulations are presented in a comparative way, mainly focusing on the potential advantages and criticisms arising from the use of single- or double-stenting procedures and of conventional or dedicated devices.

Methods

In the present study, a sequential implementation of three different numerical models, each one investigating a specific biomechanical aspect of stenting procedures in coronary bifurcations, was developed and applied.

First, a structural model simulating the stent expansions in hyperelastic coronary bifurcations¹³ was used to provide insights on the stress fields in both the arterial wall and the implanted devices. Afterwards, the realistic geometries obtained were used to investigate the haemodynamic influence of stenting procedures on the blood flow^{14,15}. Finally, the patterns of drug delivery to the lumen and the arterial walls were assessed by means of an in-house developed code¹⁶. Details regarding the numerical models have been published previously and will be summarised in the following sections to highlight their main features.

VIRTUAL BENCH TESTING

In a virtual bench test, structural analyses were implemented to simulate stenting procedures and obtain important biomechanical quantities such as stresses and deformations. This model¹³ is based on the solution of an explicit dynamics problem by means of ABAQUS/Explicit commercial code (Dassault Systemes Simulia Corp., Providence, RI, USA) and involves three main entities: a three-layered hyperelastic bifurcated artery, elastic angioplasty balloon models and elasto-plastic metallic stents (**Figure 1**). The internal diameters of the bifurcation respected the ratios proposed by the Murray law¹⁷ and were 3.28 mm, 2.78 mm and 2.44 mm for the proximal part of the MB, the distal part of the MB and the SB, respectively. The vessel wall was characterised by a constant thickness of 0.9 mm and the bifurcation angle was chosen equal to 45°. Angioplasty balloons, modelled to behave according to the typical dilation performance of semi-compliant balloons, had a diameter of 3 mm for MB and 2.5 mm for SB, respectively. The two examined stents were designed to resemble the XIENCE V DES system (Abbott Laboratories, Abbott Park, IL, USA) and the dedicated Tryton side branch BMS (Tryton Medical). Stent dimensions are shown in **Figure 1**. Positions of the devices, specific boundary conditions and pressure loads have been accurately defined in order to replicate the following stenting procedures¹⁸:

1. Provisional side branch stenting (PSB): a XIENCE V stent platform crimped to an external diameter of 1.2 mm was positioned across the bifurcation and implanted by inflating a 3 mm balloon

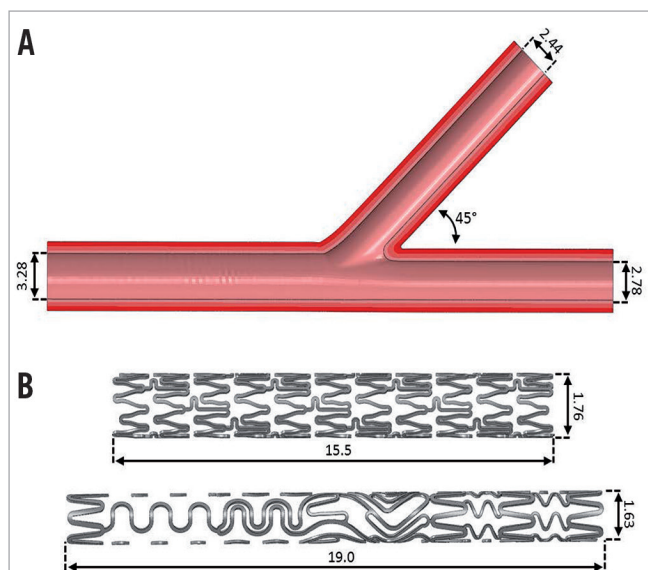


Figure 1. A) 3D model of the coronary bifurcation respecting the dimensional Murray law; B) CAD model of the two stents investigated: the conventional stent XIENCE V (top) and the dedicated device Tryton side branch stent (bottom). All measures reported are in millimetres.

- at 15 atm. After deployment, final kissing balloon (FKB) inflation was simulated by simultaneous inflation of a 3 mm balloon in the MB and a 2.5 mm balloon in the SB (accessing the SB through the more distal strut available at the SB ostium).
2. Conventional culotte (CUL): a XIENCE V stent, crimped to an external diameter of 1.2 mm, was implanted across the proximal part of the MB and the SB. Then, access to the distal MB was achieved by expanding a 3 mm balloon through side cells of the SB stent struts. Afterwards, a second XIENCE V stent was implanted in the MB across the SB take-off. The procedure was ended by a FKB inflation using a 3 mm balloon in the MB and a 2.5 mm balloon in the SB.
 3. Tryton-based culotte (TRY-CUL): the Tryton stent, crimped to an external diameter of 1.2 mm, was implanted across the proximal part of the MB and the SB. Access to the distal MB was obtained by opening the SB stent struts with a 3 mm angioplasty balloon. Then, a XIENCE V stent was implanted in the MB across the SB take-off. The procedure was ended by a FKB inflation using a 3 mm balloon in the MB and a 2.5 mm balloon in the SB¹⁹.

As an example of the virtual bench testing modelling used, the complete simulation of the Tryton-based culotte is provided in **Figure 2** and **Moving image 1**.

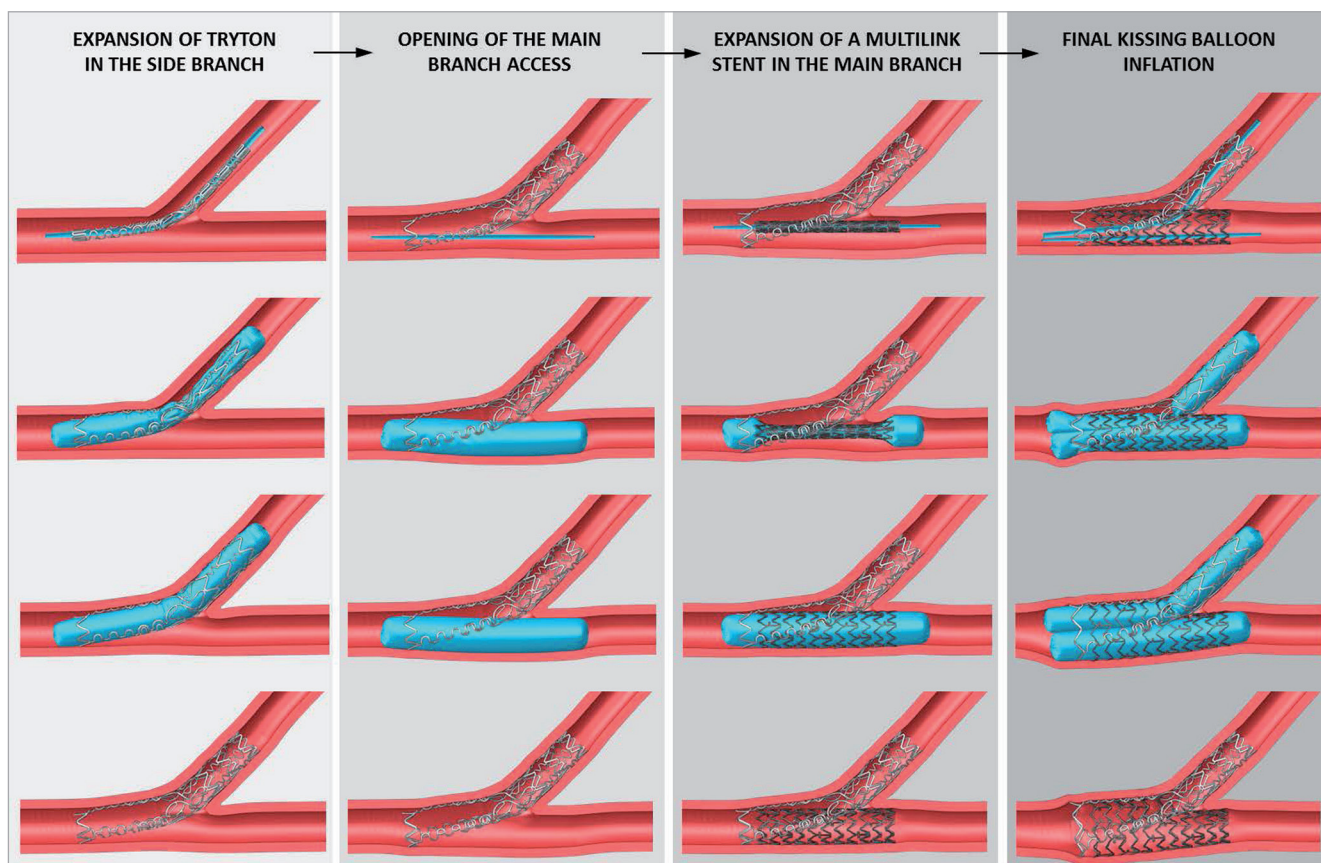


Figure 2. Virtual structural simulation of the Tryton-based culotte technique: implantation of the Tryton stent in the SB with a 2.5 mm balloon; opening of the MB using a 3 mm balloon; expansion of a conventional XIENCE V stent in the MB with a 3 mm balloon; FKB inflation performed with a 2.5 mm balloon in the SB and a 3 mm balloon in the MB.

After virtual bench testing, the metal-to-artery ratios (ratio between the total area of the external surfaces of the stents and the area) at the level of the proximal segment of the MB and the plastic equivalent deformations (PEEQ) were calculated and compared among the three investigated stenting techniques to evaluate, respectively, the effects of stent overlap and the specific stent deformations.

Additionally, since procedural pitfalls during complex bifurcation stenting procedures may play a major role, we sought to investigate the role of the SB stent rewiring site (a well-established major issue during the provisional technique) on culotte techniques. Thus, a thorough investigation of this aspect was carried out in this study. Optimal rewiring should allow the deployment of the second device and maintain free access to both branches, reducing potential procedural complications. Investigation of this issue was performed by evaluating the cross-sectional area available for an optimal rewiring in the case of the CUL and TRY-CUL techniques. Lastly, while conventional stents have a regular strut pattern, Tryton performance may be influenced by its asymmetric design, and cases of Tryton rotated by 30° and 60° (worst scenario possible) were also investigated.

A qualitative validation of such methods has been proposed in several previous studies^{6,13,20} by comparing the geometrical stented configurations obtained after virtual simulation and after *in vitro* expansions in artificial arterial models.

FLUID DYNAMICS MODEL

The final geometrical configurations obtained by virtual bench testing in the coronary bifurcation were used to create the fluid volume for CFD analyses (**Figure 3**)^{14,15}. CFD simulations were focused on near-wall analyses due to the importance of near-wall quantities on post-stenting drawbacks such as in-stent restenosis.

Blood was defined as an incompressible, non-Newtonian fluid using the Carreau model proposed by Seo et al²¹. A no-slip condition was applied between the fluid and the arterial walls which were assumed to be rigid. A transient velocity profile measured by Davies et al²² in a human left anterior descending artery was applied with a constant 70:30 flow split between the MB and SB. Assessment of the velocity field, wall shear stresses (WSS) and relative residence time (RRT)²³ in the stented regions was obtained. In particular, RRT was defined as follows:

$$RRT = \frac{1}{(1-2 \cdot OSI) \cdot TAWSS}$$

where OSI²⁴ is the oscillatory shear index and TAWSS is the time-averaged WSS. RRT can be associated to the residence time of the particles near the wall. Moreover, it has a more tangible connection to the biological mechanisms underlying atherosclerosis than WSS and OSI^{23,25}. Low WSS and high RRT are recognised as critical for the problems of both atherogenesis and in-stent restenosis^{26,27}.

DRUG-ELUTING MODELS

In complex lesions such as coronary bifurcations²⁸, understanding the capabilities of the elution of antiproliferative drugs becomes essential in the assessment of different stenting procedures. Starting from the deformed configurations obtained via structural analyses, a computational model to perform the coupled analysis of fluid dynamics and drug release was applied using an in-house code^{16,29}. The model takes into account the diffusion and dissolution mediated drug release process with a finite dissolution rate according to the equations proposed in Frenning et al³⁰. More precisely, a drug dissolves and diffuses through the interstices of the DES coating in order finally to reach the outer surface and be released. For drug transport into the arterial walls, drug diffusion

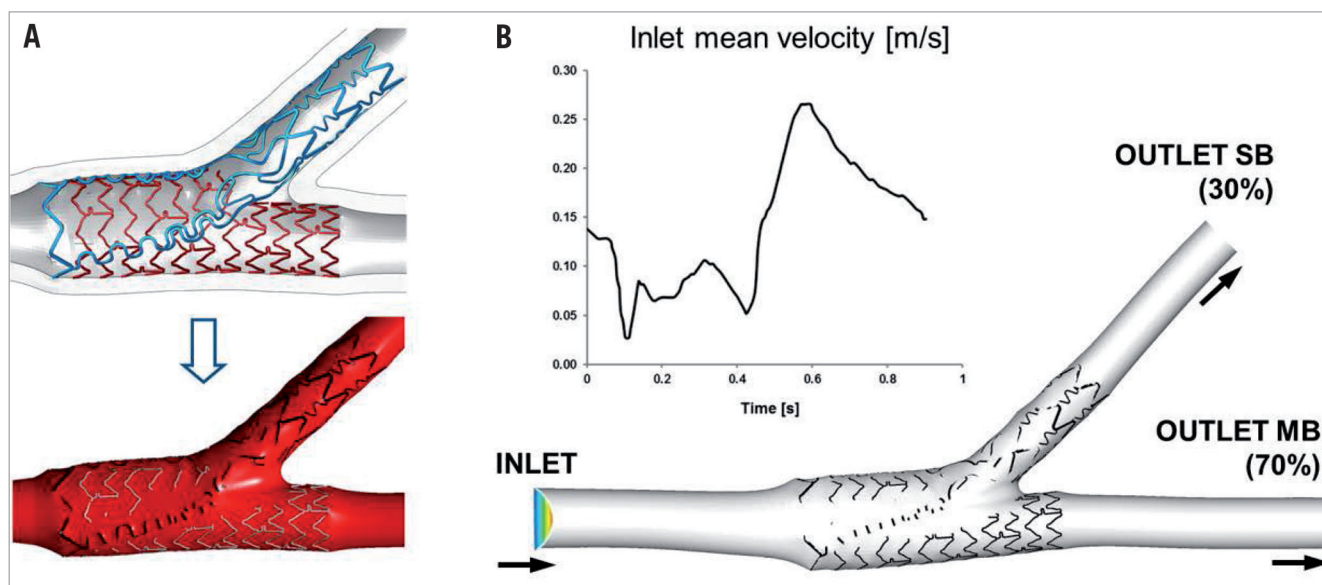


Figure 3. A) Definition of the fluid volume after the structural expansion of case 3. B) CFD model and velocity tracing applied at the inlet section of the bifurcation.

and binding as well as arterial leakage are relevant phenomena³¹. For this reason a fully coupled steady simulation of blood flow and intramural plasma filtration was performed. The obtained pressure and velocity fields were then used to perform the analysis of drug release.

According to the model proposed by D'Angelo et al³², the drug concentration inside the lumen is governed by an advection-diffusion model. Drug absorption in the arterial wall is described by means of an advection-diffusion model as for the lumen, complemented by a reaction term accounting for dynamic binding of the drug to the extracellular matrix^{33,34}. The drug diffusion coefficient refers to the release of heparin³⁵. The interplay between the drug releases into the lumen and the arterial wall is governed by interface conditions prescribing mass conservation and accounting for the selective role of the endothelial layer. For healthy tissue, the low endothelial permeability to medium/large molecules is considered to be the main barrier to intramural mass transport³⁶. The situation may be radically different in stented arteries, especially immediately after treatment and when DES are utilised, because the endothelium is severely damaged during PCI. The absence of endothelial resistance to transport is accounted for in our model by prescribing continuity of drug concentrations between the arterial lumen and the wall. For the stent struts, we assumed a squared section 0.08 mm wide (which is coherent with the selected stent platform)³⁷. As a result of that, the equivalent radius is equal to 0.052 mm. The coating consists of a polymeric film with a thickness of 7 µm. In order to evaluate the drug delivery to the arterial wall, we addressed the dose, which is defined as the time-averaged drug concentration at each point of the arterial wall, and its mean value over a given control volume. In particular, the drug doses for the whole region of the coronary bifurcation domain and for three meaningful subregions, namely the proximal part of the MB, the distal part of the MB and the SB region, were evaluated.

Results

GEOMETRICAL CONFIGURATIONS AND PHYSICAL DEFORMATIONS

Figure 4 shows the final geometrical configurations obtained at the end of virtual bench testing. Since all the simulated procedures included optimal (distal) SB rewiring and FKB inflation, all the cases resulted in patent accesses to both the MB and the SB.

Metal-to-artery ratios in the proximal region of the MB are shown in **Figure 5**. In the PSB approach only one stent is implanted resulting in a metal-to-artery ratio equal to 13.2%. On the other hand, when two conventional devices are implanted as in CUL, the ratio increases to 27.4%. In the case of TRY-CUL, the use of the dedicated stent, thanks to fewer struts in its proximal design, reduces the ratio to 20.6%.

Regarding stent deformation assessment, the maximum PEEQs obtained at the end of the procedures in the three simulated techniques are reported in **Figure 6**. In the case of PSB stenting, results showed that the maximum deformation value (0.75) is obtained in the stent strut at the ostium of the SB opened during the FKB inflation. This final step also influences the deformation state in the proximal part of the MB stent by increasing the max values of PEEQ from 0.33 to 0.43. Similar values of deformations can be found in the MB stents deployed in cases of CUL and TRY-CUL. On the other hand, looking at the plastic equivalent deformations induced in the stents implanted from the proximal MB towards the SB during the two culotte techniques, we found that the conventional stent used in CUL undergoes very high deformations in the strut opened towards the MB (0.95), while the dedicated stent used in the TRY-CUL has lower deformation overall with its higher deformation values (0.65) at the ring of struts located at its proximal end.

FLUID DYNAMIC ANALYSES: WSS AND RRT

Fluid dynamic analyses disclosed significant differences among the three investigated techniques at the level of the proximal MB.

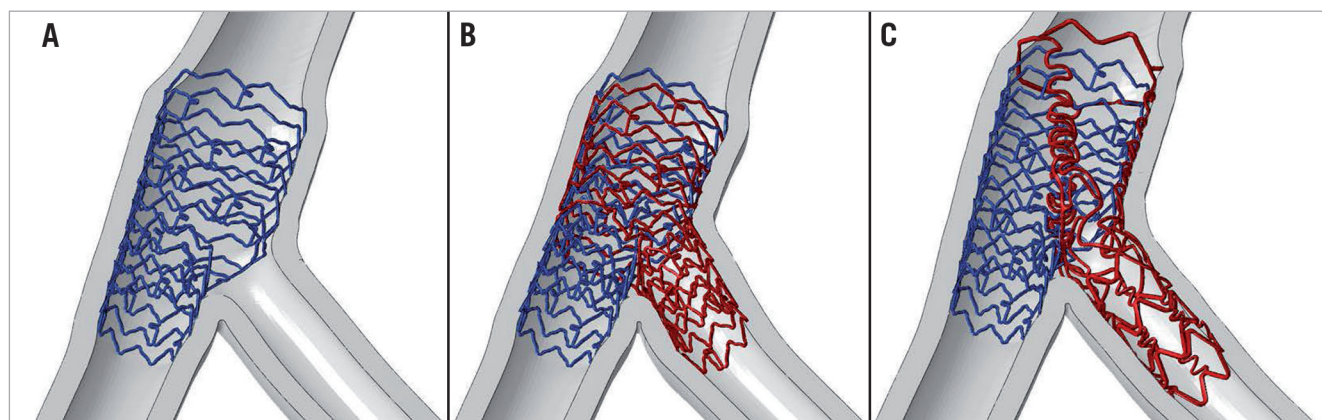


Figure 4. Final deformed geometrical configurations at the end of the three simulated procedures. A) Provisional side branch stenting (PSB); B) culotte technique performed with two conventional stents (CUL); C) culotte technique performed with a conventional XIENCE V stent in the MB and the Tryton stent in the SB (TRY-CUL).

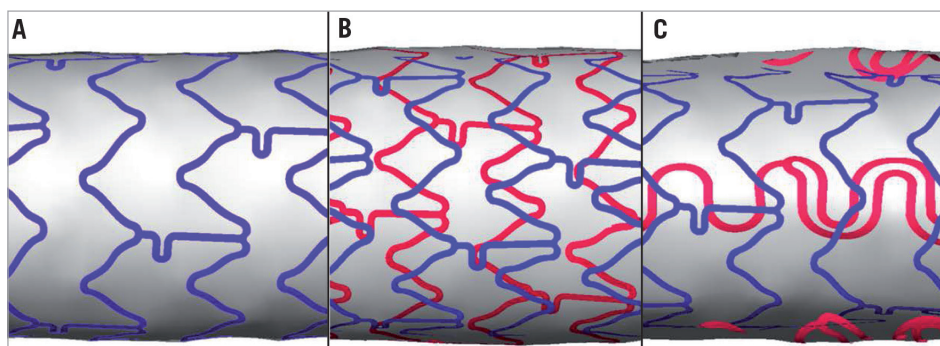


Figure 5. Metal-to-artery ratios for the three cases investigated. A) PSB, B) CUL, and C) TRY-CUL. The measured ratios in the same region of the proximal MB are 13.2%, 27.4% and 20.6%, respectively.

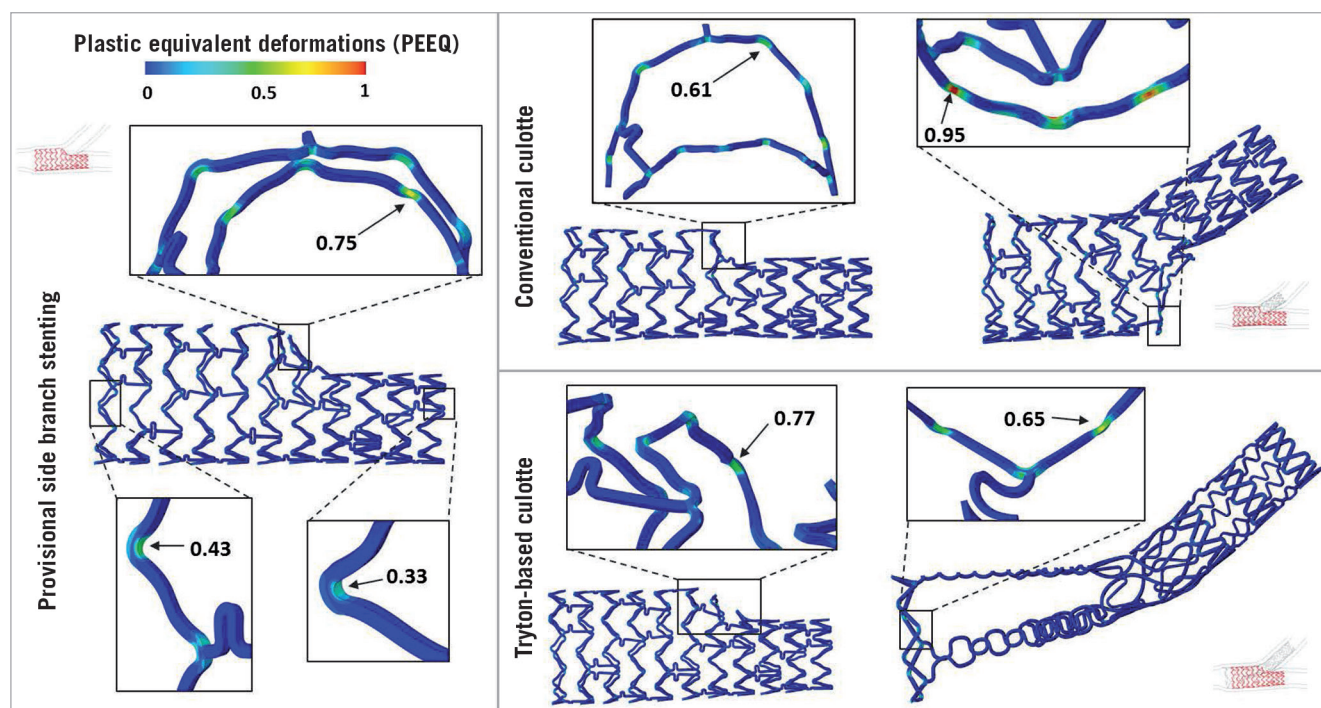


Figure 6. Comparison between the plastic equivalent deformations (PEEQ) obtained at the end of the stenting procedures in the case of PSB stenting (left), CUL (right, top) and TRY-CUL (right, bottom). Magnification areas show maximum values obtained in the implanted devices.

Figure 7 depicts the contour maps of the TAWSS (left) and RRT (right) in the three cases examined. Overall, contour maps for both parameters concordantly showed that better shear stress pattern in the proximal MB is obtained with PSB (single layer of stent struts), while the double metallic layers associated with the CUL and TRY-CUL have an adverse impact on shear stresses by enhancing the areas with low shear stress. In particular, numerical TAWSS analysis showed that the percentage areas of the proximal part of the MB characterised by TAWSS lower than 0.25 Pa were 56.0%, 88.1% and 71.6% for PSB, CUL and TRY-CUL, respectively. Similar results were obtained in the RRT analysis (**Figure 7**, numerical data not shown).

THEORETICAL DRUG ELUTION CAPABILITY

For each stenting procedure, the total amount of drug concentration in the arterial wall is reported in **Figure 8** at different time points. The drug supply to the arterial wall increases up to six hours and then a decrease is observed since the total amount of drug in the stent coating has been completely released. The mean dose was quantified and displayed in the histograms of **Figure 9** taking into consideration the different bifurcation areas. Reported graphics show that major differences in the pattern of drug release are obtained with the three investigated techniques. In particular, it is evident how drug release in the SB is only effective after the implantation of a DES. Furthermore, strut distribution and different

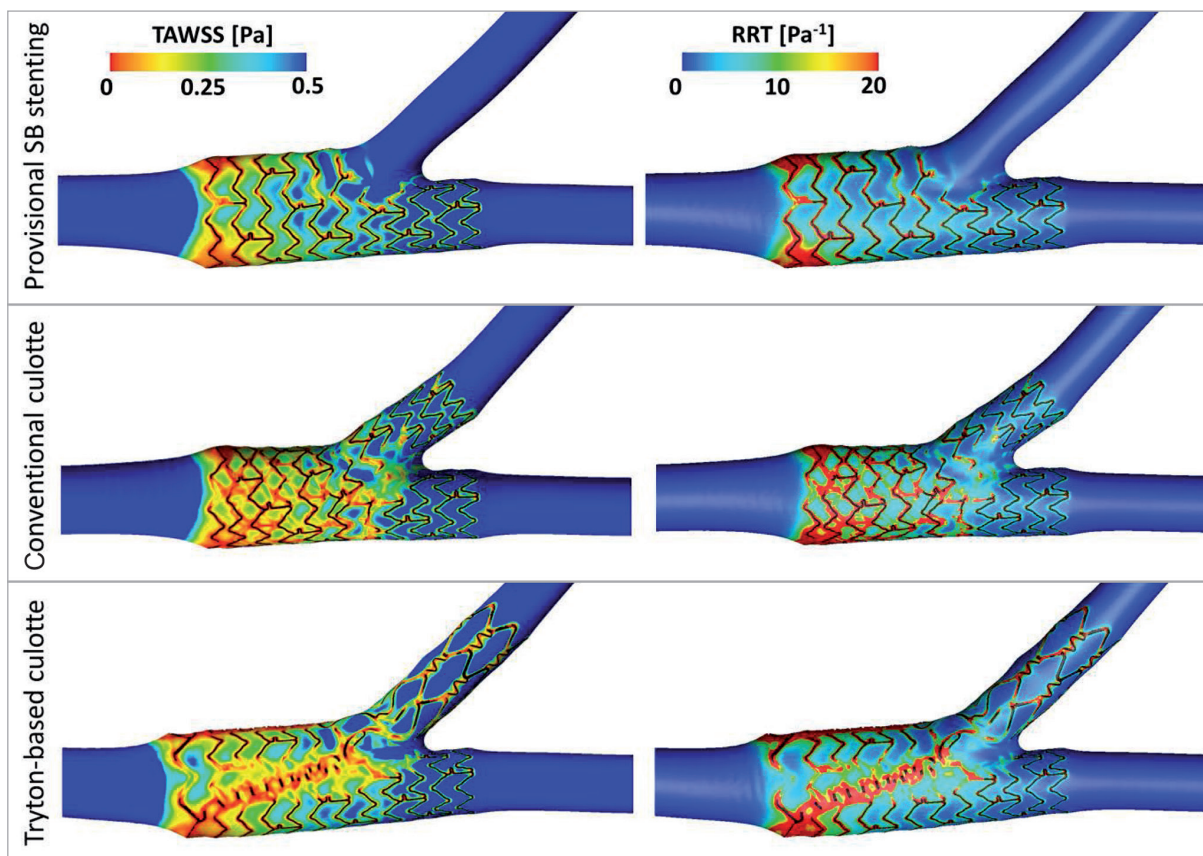


Figure 7. TAWSS and RRT contour maps. Comparison between PSB stenting (top), CUL (middle) and TRY-CUL (bottom).

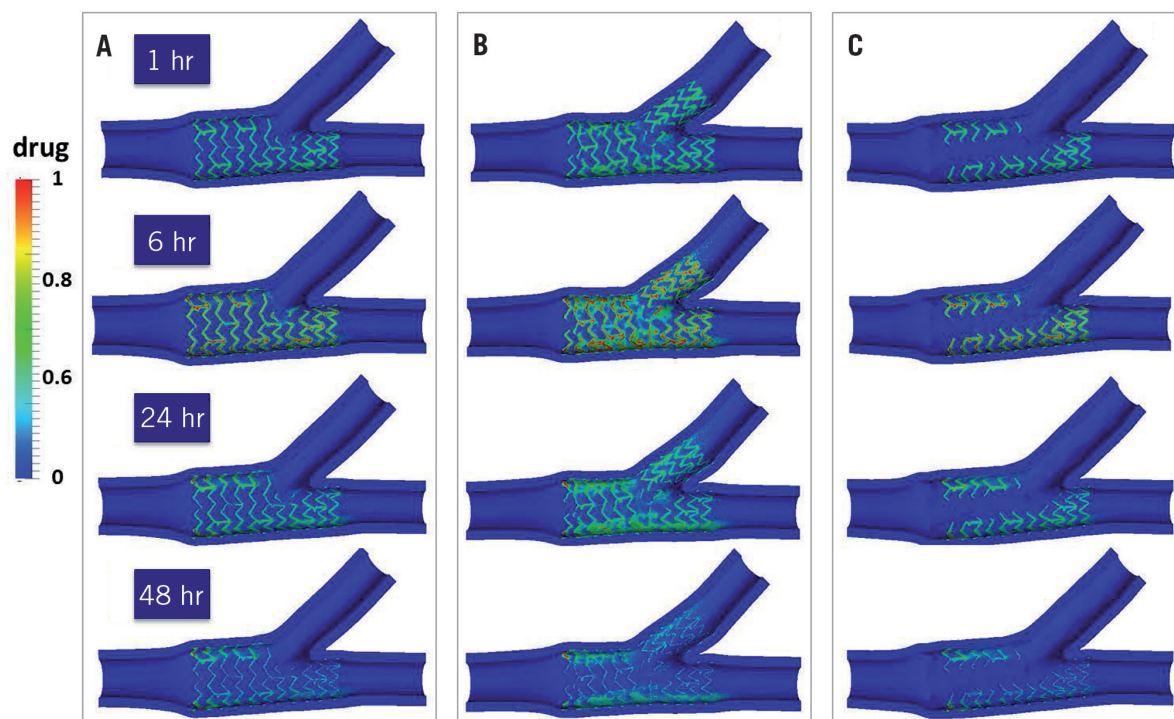


Figure 8. Drug distribution in the arterial wall of the coronary bifurcation evaluated at different time points (1 hr; 6 hr; 24 hr; 48 hr) for the PSB stenting (A), conventional CUL (B) and TRY-CUL technique (C).

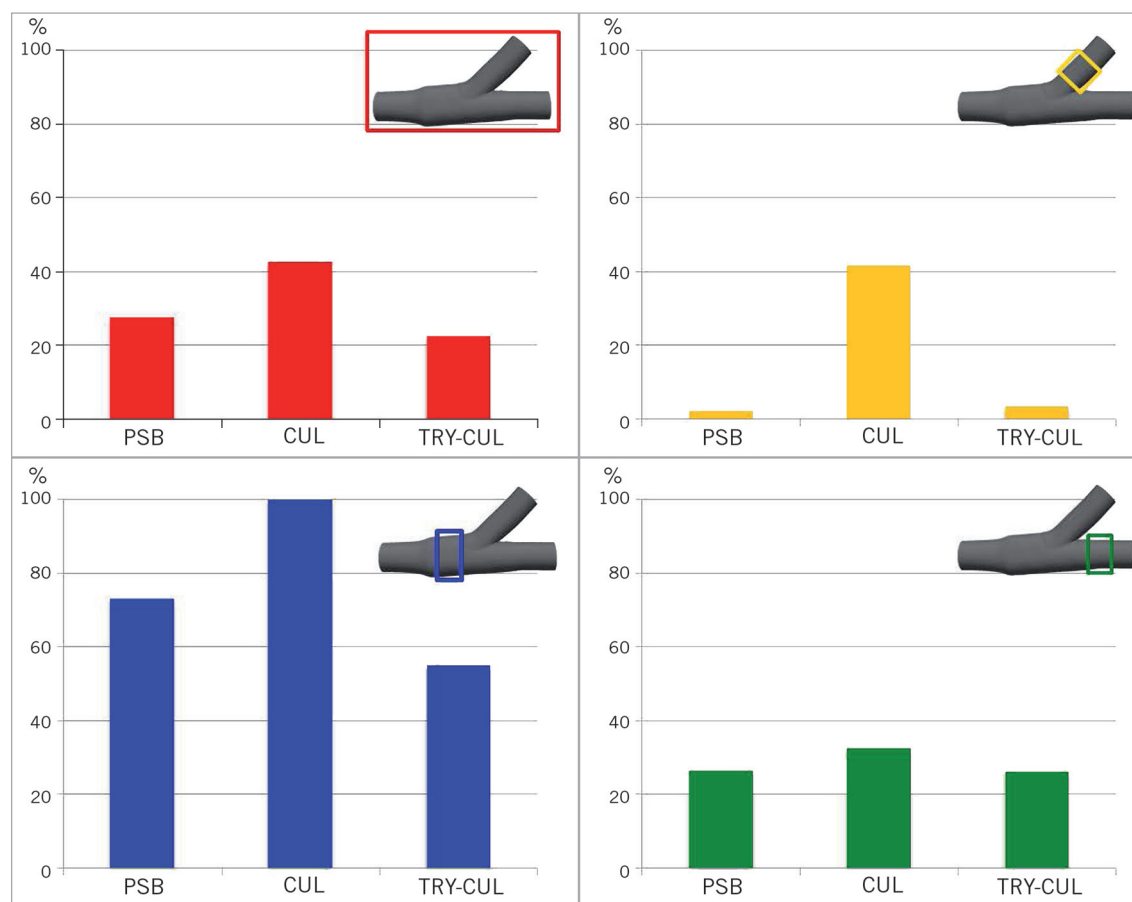


Figure 9. Mean drug dose evaluated for the whole bifurcation (red) and for the proximal (blue), distal (green) and side branch portions (yellow) for the three investigated procedures. The values are normalised with respect to the maximum value of the dose.

stent designs have been shown to affect the drug concentration in the arterial walls greatly, especially in the proximal MB where multiple metallic layers occur. The comparison of these values among PSB, conventional and Tryton-based culotte configurations is more thoroughly discussed in the next section.

SB STENT REWIRING: IMPORTANCE OF A DEDICATED DESIGN

SB stent rewiring may have a major role within culotte techniques. The available areas for optimal re-crossing of the device are equal to 8.7% after XIENCE V deployment and 59.4%, 47.6% and 40.8% for the three deployments of Tryton (ideal case, rotation 30° and rotation 60°, respectively) (Figure 10). As a consequence, the dedicated stent seems to facilitate the SB stent rewiring. In all the cases, if optimally re-crossed, the expansion of a MB balloon results in a patent access to the MB. Instead, procedural complications due to suboptimal re-crossing of a conventional stent seem to be more likely and may lead to negative geometrical and haemodynamic conditions, especially in relation to the new metallic carina (Figure 11).

Discussion

The combination of the results obtained from the three numerical models previously described provides new insights into several

aspects of the treatment of coronary bifurcations with single- or double-stenting procedures, conventional or dedicated devices. The Tryton stent is characterised by fewer struts in its proximal part and is designed to overcome some of the procedural complications which affect double-stenting techniques, such as wide double metallic layers or problematic accesses with the second device.

Firstly, a critical point of double-stenting procedures, particularly evident in the culotte techniques, is the occurrence of double or even triple metallic layers³⁸. These issues might result in higher metal-to-artery ratios, an indication of a biomechanical environment more disposed to arterial wall injuries and post-stenting complications. In this work, the three cases investigated show very different metal-to-artery ratios in the proximal part of the MB where the double metallic layer occurs (Figure 5). In particular, the PSB approach results in the lowest metal-to-artery ratio since only one stent is implanted. On the other hand, when two conventional devices are implanted as in the conventional culotte, the ratio doubles. The use of the Tryton SB stent, thanks to fewer struts in its proximal design, reduces this ratio to 20.6%. The presence of a double metallic layer has a negative influence on the haemodynamic field as well, as proved by the fluid dynamic results illustrated in Figure 7. Low values of WSS are considered as risk factors of in-stent restenosis and, as a consequence,

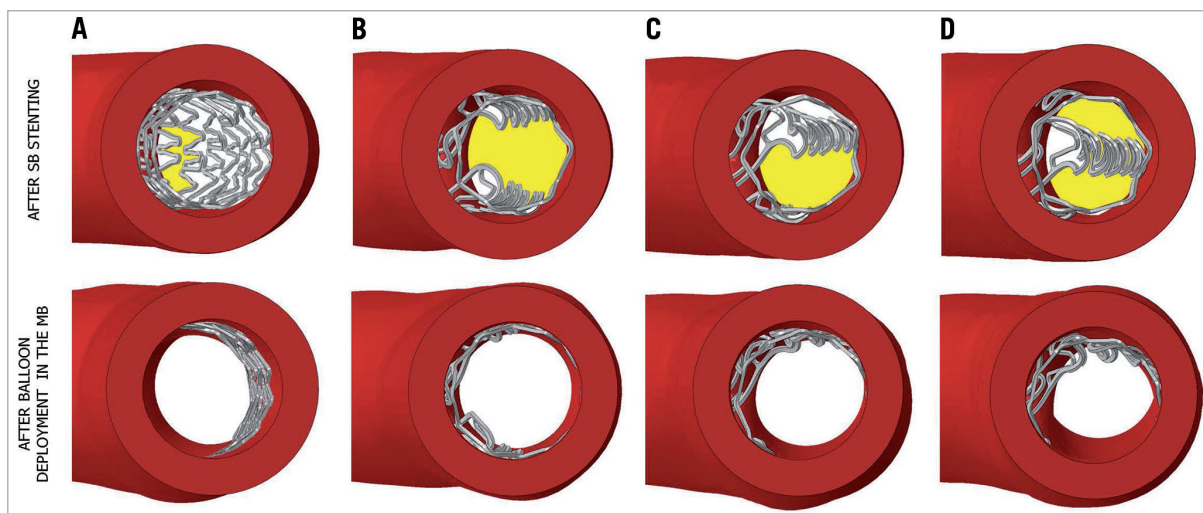


Figure 10. Top: different accesses to MB after SB stent expansion with a 2.5 mm balloon. A) Deployment of the conventional XIENCE V stent; B) implantation of the Tryton SB stent in the ideal configuration, and rotated C) at 30° and D) at 60°, the worst possible scenario. Yellow areas represent the available area for optimal re-crossing of the device and are equal to 8.7%, 59.4%, 47.6% and 40.8%, respectively. Bottom: geometrical configurations after the deployment in the MB of a 3 mm balloon.

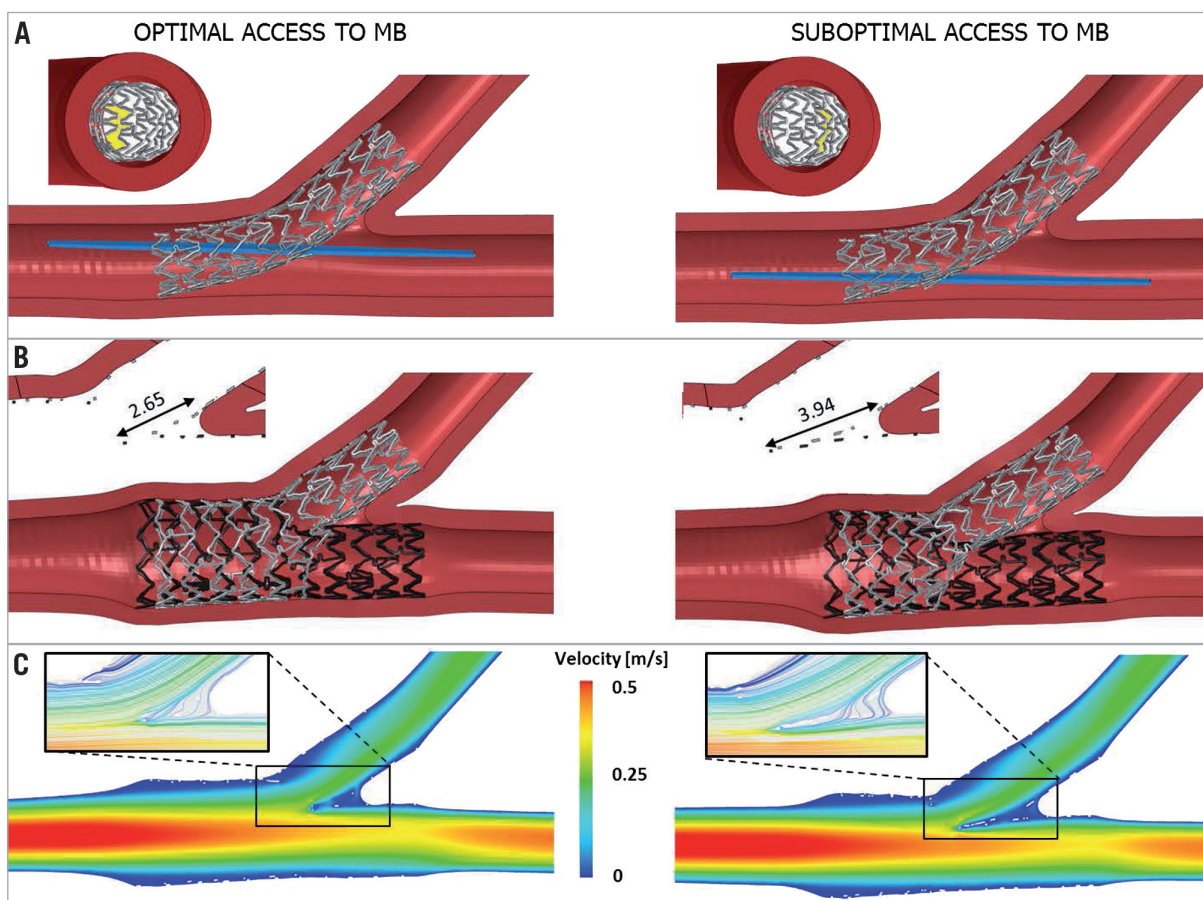


Figure 11. Comparison between an optimal and a suboptimal access to MB in the case of conventional CUL. A) Optimal (left) and suboptimal (right) crossing of the device with an angioplasty balloon. In the views from the proximal part of the MB, the crossing area is highlighted in yellow. B) Final configuration of the devices after the conventional CUL technique. A longer new metallic carina is obtained with the suboptimal access, as underlined in the close-ups of the transversal planes. C) Velocity magnitude contour maps at the maximum flow rate: in the magnification areas, the low velocities and more disturbed flow provoked by the longer metallic carina are visible.

should be avoided²⁶. TAWSS magnitude contour maps of the three cases confirm that the presence of stent struts provokes a decrease of the WSS acting on the arterial wall: this is particularly evident in the regions characterised by the overlapping of the two stents as in the case of the conventional culotte. If compared to this case, the dedicated device improves the haemodynamic conditions by decreasing the percentage of areas with low WSS from 88.1% in case 2 to 71.6%. Another critical issue is that conventional devices are designed to reach stresses and deformations that might be potentially exceeded during challenging techniques used in complex geometries such as coronary bifurcations. This occurrence might undermine the mechanical integrity of the devices. Beyond structural integrity and potential stent fracture, other important drawbacks have been related to the high deformations achieved during the expansions. Previous reports³⁹ show that very high deformations in the device might lead to structural damage and delamination of the polymer that covers the stent struts and carries antiproliferative drugs. Polymer delamination could lead to an inhomogeneous distribution of the eluted drug, disturbing the correct healing process of the artery. Indeed, structural simulations show that in all cases very high stresses and PEEQ are found in the conventional devices deployed (**Figure 6**). In particular, looking at the MB stent, high plastic deformations are found in all those stent struts rewired with a SB angioplasty balloon and opened during FKB inflations. However, these values, ranging from 0.61 to 0.77, are lower than those obtained in the case of conventional culotte after the re-crossing of the SB stent with a 3 mm balloon dilated in the MB. PEEQ values are equal to 0.95 and localise at the strut hinges close to the arterial wall opposite the bifurcation. The same step does not seem to be so critical in the case of the Tryton-based culotte since lower values of stresses and PEEQ (around 0.65) are found in the dedicated device deployed in the SB. This occurrence proves that a dedicated design might be needed to decrease the mechanical stresses and strains on the devices.

In the DES era, the capability of eluting a drug has become an essential requirement for coronary stents. Since *in vitro* or *in vivo* investigation of this aspect is technically very complex and demanding, numerical models started to be exploited and proved their ability to assess drug delivery in the arterial wall^{16,29,31}. In this work, the numerical models described in the section on drug-eluting models have been applied to the three investigated cases (**Figure 8**, **Figure 9**). The comparison among the configurations gives rise to interesting considerations. First, a higher drug dose is observed in the conventional culotte procedure with respect to the PSB, but the drug dosage is not doubled. Indeed, the incomplete stent apposition and the superposition of the struts which occurs when two stents are deployed in the proximal MB affect the optimal release of a drug to the arterial wall causing drug loss in the blood stream. This occurrence was quantitatively demonstrated by Foin et al⁴⁰ through experimental measurements on *in vitro* stent expansions. In that study, the authors proved that a conventional CUL technique led to a higher rate of strut malappositions (39.1±10.7%) as opposed to a T-TAP procedure (4.2±7.2%) where no stent overlapping occurs. Concerning the SB region, significant drug supply seems to be

provided only in the case when the SB is treated by means of a DES (conventional culotte). A small supply of drug in the SB is observed in the other cases and it is probably due to the flow-mediated drug transport. The use of a dedicated BMS in the SB guarantees the re-opening of the stenotic area but does not seem to be able to supply a sufficient amount of drug to the SB. These results are in agreement with the considerations by Grundeken et al², who suggested that further improvements might be achieved by coating these dedicated SB devices with a drug, with the aim of not only providing an optimal ostial scaffolding of the SB but also minimising the in-stent restenosis. Moreover, the presence of bare metal struts in the proximal segment of the MB seems to influence the pattern of drug release at this level after TRY-CUL.

Lastly, it is quite reasonable to assume that suboptimal procedural outcomes could increase the potential risks of post-stenting clinical complications such as in-stent restenosis or thrombosis. Above all, double-stenting procedures seem to be more prone to procedural errors mainly due to their technical complexity. In particular, within the culotte techniques a critical point is the crossing of the first device implanted with an angioplasty balloon that enlarges the stent struts and allows the advancement of the second device in the other branch. An optimal balloon insertion should cross the SB stent close to the bifurcation to let the struts adhere to the arterial wall opposite the bifurcation without hindering the SB access. Looking at the virtual bench test results in **Figure 10**, it is clear that the dedicated stent provides a wider area (59.4%) available for an optimal re-crossing (**Figure 10B**) if compared to the standard stent (8.7%) (**Figure 10A**). Moreover, the highly regular structure of the conventional stent makes the optimal crossing area slightly affected by the uncontrollable rotation of the device. On the other hand, a suboptimal procedure performed with the Tryton stent rotated to 30° (**Figure 10C**) and 60° (worst scenario) (**Figure 10D**) reduces the optimal crossing area to 47.6% and 40.8%, respectively, still enhancing the performance of the conventional device examined. In all these cases, the MB balloon inflation which followed resulted in a completely patent access to the MB (**Figure 10**, bottom), thus making rotational alignment of the Tryton SB stent a trivial point. Accordingly, the use of a dedicated device seems to have a lower chance of procedural complications due to suboptimal SB stent rewiring. On the other hand, suboptimal rewiring of a conventional SB stent seems to be more probable and, when it occurs, may lead to negative geometrical and haemodynamic conditions. For instance, **Figure 11** provides a comparison between an optimal conventional CUL technique (**Figure 11**, left) and an example of suboptimal procedure obtained crossing the stent struts far from the bifurcation (**Figure 11**, right). In the second case, the result of the MB balloon deployment is a patent MB ostium but a problematic access to the SB caused by the presence of several stent struts. In this way, after MB stent deployment, FKB inflation could only be performed with a proximal access to the SB, leading to a greater new metallic carina. Results in terms of geometrical configuration and haemodynamic influence at the end of the whole procedure are visible in **Figure 11B** and **Figure 11C**, respectively. In particular,

differences can be found looking at the longer new metallic carina obtained in the suboptimal case (3.95 mm) as opposed to the optimal one (2.65 mm). This new metallic carina has a great influence on the haemodynamic field as proved by the CFD results shown in **Figure 11C**. In particular, a wider area of low velocities and recirculations is visible close to the bifurcation. Recently, this issue obtained increased interest in the clinical field as it has been associated with delayed healing and a major risk of thrombotic events⁴¹. Our findings are in agreement with recent studies, such as those presented by Foin et al^{40,42}, where CFD simulations based on *in vitro* expansions of stents in polymeric silicone models were performed. Lastly, in the suboptimal case, slight increases in the mechanical stresses and strains on the devices in terms of Von Mises stress and plastic deformations at the maximum expansion were also found.

Study limitations

Despite their continuous improvements and development, numerical models are still affected by a number of limitations that need to be overcome to replicate *in vivo* clinical conditions. In this light, the results herein presented should be carefully interpreted when drawing any clinical conclusion and the values should not be considered as absolute but only used for comparative assessment of different cases. In the following paragraph, a list of the major assumptions made is provided:

- Artery: the materials used to define its mechanical behaviour did not consider its anisotropic and inhomogeneous nature. Moreover, the geometries used in this work had realistic dimensions but represented idealised models.
- Atherosclerotic plaques were not included in the model.
- Stent models could differ slightly from the actual commercial devices both in terms of geometry and materials. In particular, a common medical Co-Cr alloy was used for all the devices even if each stent is characterised by a typical alloy whose specific composition and treatment is most of the time unknown. Moreover, no data were available for the exact behaviour of the drug coating in terms of drug composition and drug release. Lastly, only a single conventional stent was investigated.
- No image-based reconstructions were used. Indeed, the models implemented could not provide patient-specific indications but only general guidelines which must be carefully interpreted and adapted to every specific clinical case.

Lastly, validation is currently the major issue for biomechanical numerical models. A direct validation is not straightforward, mainly due to the lack of experimental studies on stenting procedures, especially regarding the CFD and drug elution models. Difficulties in measuring haemodynamic and drug transport quantities together with the complexity and small dimensions of metallic stents strongly limit both *in vivo* and *in vitro* experimental studies. As a consequence, only some indirect qualitative comparisons among numerical simulations and *in vitro* expansions of metallic stents have been proposed in the recent literature and certainly in the near future great efforts should be dedicated to overcome this issue.

Conclusions

This work shows how numerical models might successfully complement the information on stenting procedures obtained with traditional approaches such as *in vitro* bench testing or clinical trials. Their ability to provide direct information on clinically interesting biomechanical variables such as mechanical stresses in the artery and the stents could facilitate the design process of the devices and clinical planning. In particular, this work confirmed that new dedicated devices, still requiring some improvements in their design and concept, might be an interesting opportunity when stenting coronary bifurcation lesions.

Funding

The authors have been supported by the Grant “Nanobiotechnology: Models and methods for degradable materials” of the Italian Institute of Technology (IIT). E. Cutri, L. Formaggia and P. Zunino are also supported by the European Research Council Advanced Grant “Mathcard, Mathematical Modelling and Simulation of the Cardiovascular System”, Project ERC-2008-AdG 227058. S. Morlacchi, C. Chiastra, G. Dubini and F. Migliavacca are also supported by the European Commission under the 7th Framework Programme, within the project “RT3S - Real Time Simulation for Safer vascular Stenting”.

Impact on daily practice

The present study gives evidence of the additional knowledge made available by computational reconstructions of DES implantation in bifurcated coronary segments. We showed how different techniques with standard DES or Tryton stents are associated with different patterns of stent strut distribution, shear stress and drug elution at the level of the treated bifurcation. Of note, Tryton-facilitated culotte, as compared with culotte with two DES, is associated with a lower metal-to-artery ratio, but has no significant drug elution into the side branch. Furthermore, both conventional culotte and Tryton-based culotte techniques have a final strut distribution which is dependent on stent orientation during placement and side branch rewiring before kissing. All these aspects may theoretically play a role in determining the clinical outcome of patients undergoing percutaneous coronary intervention on bifurcations. Moreover, these technical aspects are usually not considered during bifurcation interventions and may be checked in clinical practice by using the latest generation non-invasive imaging modalities, such as optical coherence tomography.

Conflict of interest statement

The authors have no conflicts of interest to declare.

References

1. Hildick-Smith D, Lassen JF, Albiero R, Lefevre T, Darremont O, Pan M, Ferenc M, Stankovic G, Louvard Y. Consensus from the 5th European Bifurcation Club meeting. *EuroIntervention*. 2010;6:34-8.

2. Grundeken MJ, Stella PR, Wykrzykowska JJ. Why the provisional single-stent approach is not always the right strategy; arguments for the development of dedicated bifurcation devices. *EuroIntervention*. 2012;7:1249-53.
3. Magro M, Wykrzykowska J, Serruys PW, Simsek C, Nauta S, Lesiak M, Stanislawska K, Onuma Y, Regar E, van Domburg RT, Grajek S, Geuns RJ. Six-month clinical follow-up of the Tryton side branch stent for the treatment of bifurcation lesions: a two center registry analysis. *Catheter Cardiovasc Interv*. 2011;77:798-806.
4. Agostoni P, Foley D, Lesiak M, Belkacemi A, Dens J, Kumsars I, Scott B, Oemrawsingh P, Dubois C, Garcia E, Lefèvre T, Stella PR. A prospective multicentre registry, evaluating real-world usage of the Tryton side branch stent: results of the E-Tryton 150/Benelux registry. *EuroIntervention*. 2012;7:1293-300.
5. Capelli C, Gervaso F, Petrini L, Dubini G, Migliavacca F. Assessment of tissue prolapse after balloon expandable stenting: influence of stent cell geometry. *Med Eng Phys*. 2009;31:441-7.
6. Mortier P, De Beule M, Segers P, Verdonck P, Verheghe B. Virtual bench testing of new generation coronary stents. *EuroIntervention*. 2011;7:369-76.
7. Mortier P, De Beule M. Stent design back in the picture: an engineering perspective on longitudinal stent compression. *EuroIntervention*. 2011;7:773-5.
8. Harewood F, Grogan J, McHugh PE. A multiscale approach to failure assessment in deployment for cardiovascular stents. *Journal of Multiscale Modelling*. 2011;2:1-22.
9. Morlacchi S, Keller B, Arcangeli P, Balzan M, Migliavacca F, Dubini G, Gunn J, Arnold N, Narracott A, Evans D, Lawford P. Hemodynamics and in-stent restenosis: micro-CT images, histology, and computer simulations. *Ann Biomed Eng*. 2011;39:2615-26.
10. Williams AR, Koo BK, Gundert TJ, Fitzgerald PJ, LaDisa JF Jr. Local hemodynamic changes caused by main branch stent implantation and subsequent virtual side branch balloon angioplasty in a representative coronary bifurcation. *J Appl Physiol*. 2010;109:532-40.
11. Ellwein LM, Otake H, Gundert TJ, Koo BK, Shinke T, Honda Y, Shite J, LaDisa JF. Optical Coherence Tomography for Patient-specific 3D Artery Reconstruction and Evaluation of Wall Shear Stress in a Left Circumflex Coronary Artery. *Cardiov Eng Technol*. 2011;2:212-27.
12. Kolachalama VB, Tzafiriri AR, Arifin DY, Edelman ER. Luminal flow patterns dictate arterial drug deposition in stent-based delivery. *J Control Release*. 2009;133:24-30.
13. Gastaldi D, Morlacchi S, Nichetti R, Capelli C, Dubini G, Petrini L, Migliavacca F. Modelling of the provisional side-branch stenting approach for the treatment of atherosclerotic coronary bifurcations: effects of stent positioning. *Biomech Model Mechanobiol*. 2010;9:551-61.
14. Morlacchi S, Chiastra C, Gastaldi D, Pennati G, Dubini G, Migliavacca F. Sequential structural and fluid dynamic numerical simulations of a stented bifurcated coronary artery. *J Biomech Eng*. 2011;133:121010.
15. Chiastra C, Morlacchi S, Pereira S, Dubini G, Migliavacca F. Computational fluid dynamics of stented coronary bifurcations studied with a hybrid discretization method. *Eur J Mech B/Fluids*. 2012;35:76-84.
16. Cutri E, Zunino P, Morlacchi S, Chiastra C, Migliavacca F. Drug delivery patterns for different stenting techniques in coronary bifurcations: a comparative computational study. *Biomech Model Mechanobiol*. 2013;12:657-69.
17. Murray CD. The Physiological Principle of Minimum Work: I. The Vascular System and the Cost of Blood Volume. *Proc Natl Acad Sci U S A*. 1926;12:207-14.
18. Louvard Y, Thomas M, Dzavik V, Hildick-Smith D, Galassi AR, Pan M, Burzotta F, Zelizko M, Dudek D, Ludman P, Sheiban I, Lassen JF, Darremont O, Kastrati A, Ludwig J, Iakovou I, Brunel P, Lansky A, Meerkin D, Legrand V, Medina A, Lefèvre T. Classification of coronary artery bifurcation lesions and treatments: time for a consensus! *Catheter Cardiovasc Interv*. 2008;71:175-83.
19. Kaplan AV, Davis HR. Tryton side-branch stent. *EuroIntervention*. 2006;2:270-1.
20. Conti M, Van Loo D, Auricchio F, De Beule M, De Santis G, Verheghe B, Pirrelli S, Otero A. Impact of carotid stent cell design on vessel scaffolding: a case study comparing experimental investigation and numerical simulations. *J Endovasc Ther*. 2011;18:397-406.
21. Seo T, Schachter LG, Barakat AI. Computational study of fluid mechanical disturbance induced by endovascular stents. *Ann Biomed Eng*. 2005;33:444-56.
22. Davies JE, Whinnett ZI, Francis DP, Manisty CH, Aguado-Sierra J, Willson K, Foale RA, Malik IS, Hughes AD, Parker KH, Mayet J. Evidence of a dominant backward-propagating "suction" wave responsible for diastolic coronary filling in humans, attenuated in left ventricular hypertrophy. *Circulation*. 2006;113:1768-78.
23. Himgburg HA, Grzybowski DM, Hazel AL, LaMack JA, Li XM, Friedman MH. Spatial comparison between wall shear stress measures and porcine arterial endothelial permeability. *Am J Physiol Heart Circ Physiol*. 2004;286:H1916-22.
24. Ku DN, Giddens DP, Zarins CK, Glagov S. Pulsatile flow and atherosclerosis in the human carotid bifurcation. Positive correlation between plaque location and low and oscillating shear stress. *Arteriosclerosis*. 1985;5:293-302.
25. Lee SW, Antiga L, Steinman DA. Correlations among indicators of disturbed flow at the normal carotid bifurcation. *J Biomech Eng*. 2009;131:061013.
26. Malek AM, Alper SL, Izumo S. Hemodynamic shear stress and its role in atherosclerosis. *J Am Med Ass*. 1999;282:2035-42.
27. Hoi Y, Zhou Y, Zhang X, Henkelman X, Steinman DA. Correlation between local hemodynamics and lesion distribution in a novel aortic regurgitation murine model of atherosclerosis. *Ann Biomed Eng*. 2011;39:1414-22.
28. Morice M, Serruys PW, Eduardo Sousa J, Fajadet J, Hayashi EB, Perin M, Colombo A, Schuler G, Barragan P, Guagliumi G, Molnar F, Falotico R. A randomized comparison of a sirolimus-eluting stent with a standard stent for coronary revascularization. *N Engl J Med*. 2002;346:1773-80.
29. D'Angelo C, Zunino P, Porpora A, Morlacchi S, Migliavacca F. Model reduction strategies enable computational analysis of

controlled drug release from cardiovascular stents. *SIAM J Appl Math.* 2012;71:2312-33.

30. Frenning G. Theoretical investigation of drug release from planar matrix systems: effects of a finite dissolution rate. *J Control Release.* 2003;92:331-9.

31. Balakrishnan B, Tzafriri AR, Seifert P, Groothuis A, Rogers C, Edelman ER. Strut position, blood flow, and drug deposition, implications for single and overlapping drug-eluting stents. *Circulation.* 2005;111:2958-65.

32. D'Angelo C, Zunino P. Robust numerical approximation of the coupled Stokes' and Darcy's flows applied to vascular hemodynamics and biochemical transport. *Esaim Math Model Numer Anal.* 2011;45:447-76.

33. Sakharov DV, Kalachev LV, Rijken DC. Numerical simulation of local pharmacokinetics of a drug after intravascular delivery with an eluting stent. *J Drug Target.* 2002;10:507-13.

34. Levin AD, Edelman ER. Diffusion-limited binding explains binary dose response for local arterial and tumour drug delivery. *Cell Prolif.* 2009;42:348-63.

35. Hwang CW, Wu D, Edelman ER. Physiological transport forces govern drug distribution for stent-based delivery. *Circulation.* 2001;104:600-5.

36. Prosi M, Zunino P, Perktold K, Quarteroni A. Mathematical and numerical models for transfer of low-density lipoproteins through the arterial walls: a new methodology for the model set up with applications to the study of disturbed luminal flow. *J Biomech.* 2005;38:903-17.

37. Sheiban I, Villata G, Bollati M, Sillano D, Lotrionte M, Biondi-Zoccai G. Next-generation drug-eluting stents in coronary artery disease: focus on everolimus-eluting stent (Xience V). *Vasc Health Risk Manag.* 2008;4:31-8.

38. Latib A, Colombo A. Bifurcation disease: what do we know, what should we do? *JACC Cardiovasc Interv.* 2008;1:218-26.

39. Guérin P, Pilet P, Finet G, Gouëffic Y, N'Guyen JM, Crochet D, Tijou I, Pacaud P, Loirand G. Drug-eluting stents in bifurcations: bench study of strut deformation and coating lesions. *Circ Cardiovasc Interv.* 2010;3:120-6.

40. Foin N, Alegria-Barrero E, Torii R, Chan PH, Viceconte N, Davies JE, Di Mario C. Crush, culotte, T and protrusion: which 2-stent technique for treatment of true bifurcation lesions? - insights from in vitro experiments and micro-computed tomography. *Circ J.* 2013;77:73-80.

41. Nakazawa G, Yazdani SK, Finn AV, Vorpahl M, Kolodgie FD, Virmani R. Pathological findings at bifurcation lesions: the impact of flow distribution on atherosclerosis and arterial healing after stent implantation. *J Am Coll Cardiol.* 2010;55:1679-87.

42. Foin N, Torii R, Mortier P, De Beule M, Viceconte N, Chan PH, Davies JE, Xu XY, Krams R, Di Mario C. Kissing balloon or sequential dilation of the side branch and main vessel for provisional stenting of bifurcations: lessons from micro-computed tomography and computational simulations. *JACC Cardiovasc Interv.* 2012;5:47-56.

Online data supplement

Moving image 1. Animation of the Tryton-based culotte technique. 1) Deployment of the Tryton stent with a 2.5 mm balloon across the bifurcation; 2) inflation of a 3 mm balloon through the side branch stent struts in order to free the access to the distal part of the main branch; 3) implantation of a XIENCE V stent in the main branch by deployment of a 3 mm balloon; 4) final kissing balloon inflation.